AD-A066 198 VIRGINIA POLYTECHNIC INST AND STATE UNIV BLACKSBURG F/G 20/4
FLOW VISUALIZATION OF TRANSIENT AND OSCILLATORY SEPARATING LAMI--ETC(U)
1978 D P TELIONIS, C P KOROMILAS DAHC04-75-G-0067
UNCLASSIFIED ARO-12680.6-E NL

1 OF 1
AD
A066198

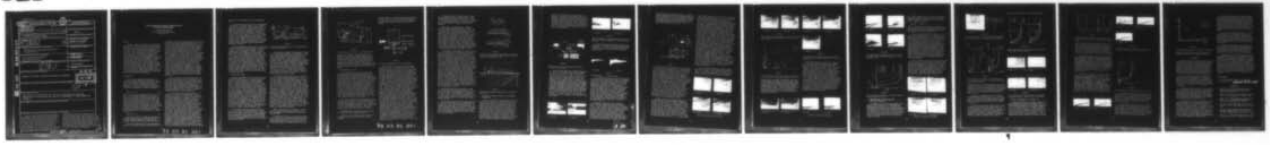

END
DATE
FILMED
5-79
DDC

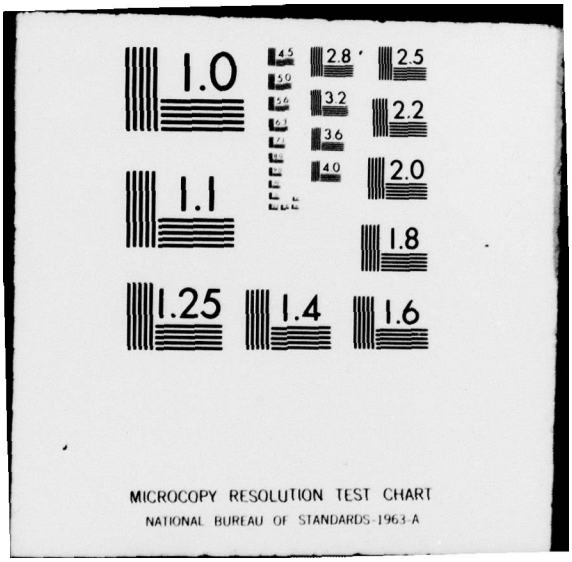
1.0
1.1
1.25
1.4
1.6
1.8
2.0
2.2
2.5
2.8
3.2
3.6
4.0
4.5
5.0
5.6
MICROCOPY RESOLUTION TEST CHART
NATIONAL BUREAU OF STANDARDS-1963-A

Unclassified

SECURITY CLASSIFICATION OF THIS PAGE (When Data Entered)

(18) ARO

REPORT DOCUMENTATION PAGE

(2)

READ INSTRUCTIONS BEFORE COMPLETING FORM

1. REPORT NUMBER (19) 12680.6-E	2. GOVT ACCESSION NO.
3. RECIPIENT'S CATALOG NUMBER	
4. TITLE (and Subtitle) (6) FLOW VISUALIZATION OF TRANSIENT AND OSCILLATORY SEPARATING LAMINAR FLOWS	5. TYPE OF REPORT & PERIOD COVERED: Reprint
	6. PERFORMING ORG. REPORT NUMBER
7. AUTHOR(s) (10) D. P. Telionis, C. P. Koromilas	8. CONTRACT OR GRANT NUMBER(s) (15) DAHC04-75-G-0067
9. PERFORMING ORGANIZATION NAME AND ADDRESS: VA Polytechnic Institute and State U, Blacksburg, VA	10. PROGRAM ELEMENT, PROJECT, TASK AREA & WORK UNIT NUMBERS
11. CONTROLLING OFFICE NAME AND ADDRESS: U. S. Army Research Office, Post Office Box 12211, Research Triangle Park, NC 27709	12. REPORT DATE (11) 1978
	13. NUMBER OF PAGES: 12
14. MONITORING AGENCY NAME & ADDRESS (if different from Controlling Office) (12) 13p.	15. SECURITY CLASS. (of this report): Unclassified
	15a. DECLASSIFICATION/DOWNGRADING SCHEDULE

16. DISTRIBUTION STATEMENT (of this Report)

Approved for public release; distribution unlimited.

DDC RECEIVED MAR 19 1979 B

17. DISTRIBUTION STATEMENT (of the abstract entered in Block 20, if different from Report)

18. SUPPLEMENTARY NOTES

The findings in this report are not to be construed as an official Department of the Army position, unless so designated by other authorized documents.

19. KEY WORDS (Continue on reverse side if necessary and identify by block number)

20. ABSTRACT (Continue on reverse side if necessary and identify by block number)

Unsteady laminar viscous flows are investigated experimentally. Special attention is directed towards the response of separation to impulsive or oscillatory changes of the pressure gradient. Experiments are performed in water tunnels constructed especially for this study. Water or glycerin-water mixtures are used to achieve low Reynolds numbers with not so small actual velocities. The method of measurement is essentially based on visualization techniques, especially developed for this investigation. The results confirm earlier analytical and experimental evidence that upstream of the point of separation, a thin reversed flow layer may exist or equivalently, that zero skin friction is not a proper criterion of separation for unsteady flows. The criterion of Despard and Miller for oscillatory flows is proved to be valid for the few cases of oscillations considered here. For transient flows the problem is more complex. The present data may offer some physical insight on transient separation and may eventually lead to appropriate theoretical modeling of the pheromenon.

DD 1 JAN 73 1473 EDITION OF 1 NOV 65 IS OBSOLETE

407206

Unclassified

SECURITY CLASSIFICATION OF THIS PAGE (When Data Entered)

AD A066198

DDC FILE COPY

FLOW VISUALIZATION OF TRANSIENT AND OSCILLATORY SEPARATING LAMINAR FLOWS

D. P. Telionis and C. P. Koromilas
Virginia Polytechnic Institute and State University
Blacksburg, Virginia

ABSTRACT

Unsteady laminar viscous flows are investigated experimentally. Special attention is directed towards the response of separation to impulsive or oscillatory changes of the pressure gradient. Experiments are performed in water tunnels constructed especially for this study. Water or glycerin-water mixtures are used to achieve low Reynolds numbers with not so small actual velocities. The method of measurement is essentially based on visualization techniques, especially developed for this investigation. The results confirm earlier analytical and experimental evidence that upstream of the point of separation, a thin reversed flow layer may exist or equivalently, that zero skin friction is not a proper criterion of separation for unsteady flows. The criterion of Despard and Miller for oscillatory flows is proved to be valid for the few cases of oscillations considered here. For transient flows the problem is more complex. The present data may offer some physical insight on transient separation and may eventually lead to appropriate theoretical modeling of the phenomenon.

INTRODUCTION

One of the most important characteristics of viscous flow is the phenomenon of separation. This term in the language of aerodynamics means the breakaway of the flow from a bounding surface and the initiation of a wake. For the case of steady two-dimensional or axisymmetric flow over fixed walls, a criterion for separation was suggested by Prandtl [1]

$$\frac{\partial u}{\partial y} = 0 \text{ at } y = 0 \qquad (1)$$

where u is the velocity component parallel to the wall and y is the coordinate perpendicular to the wall. This criterion proved to predict the phenomenon correctly and it has been used extensively by both theoreticians and experimentalists for over fifty years. However, Sears [2] Moore [3], and Rott [4, 5], demonstrated that Prandtl's criterion (Eq. (1)) is inadequate for cases other than steady flow over fixed walls and indicated the need for a generalized definition and a convenient criterion for separation. They also suggested independently a more appropriate criterion for the case of steady flow over moving walls, namely (see Fig. 1.2)

$$\frac{\partial u}{\partial y} = 0 \text{ at } u = 0 \qquad (2)$$

Sears [2] and Moore [3] proposed a definition of unsteady separation which is essentially equivalent to the above condition (equation (2)) expressed in a coordinate system moving with the point of separation.

Vidal [6] and later Ludwig [7] performed experiments with a cylinder rotating in the test section of a wind tunnel. Using hot wire anemometers, they were able to verify the theoretical model of equation (2) at least for the case of downstream moving walls. Tennant and his associates (Tennant and Yang, [8]; Tennant, [9]) also performed experiments with moving boundaries for both laminar and turbulent flow. Their findings pertain to skin velocities much larger than the free stream and always downstream motion of the skin. Despard and Miller [10] again inspired by the analytical work of Moore [3] for laminar flow and the experimental work of Sandborn [11] for turbulent flow, considered the problem of an oscillating outer flow velocity and proposed a definition for a mean location of separation. Working with air and using hot wire anemometers, they were also able to verify that in unsteady flow the location of zero skin friction is not necessarily related to the phenomenon of separation. In a very recent effort, Simpson [12] and Kenison [13] investigated experimentally the neighborhood of separation of an oscillating turbulent boundary layer. Kenison reports that as separation is approached, fluctuating velocity overshoots and phase angles indicate sharp changes. However, the basic features of oscillating turbulent separation are similar to those of laminar separation.

Telionis and Werle [14] showed analytically that for steady boundary-layer flow over moving walls, the location of zero skin friction is nonsingular, while a typical separation singularity appears at the station where Moore, Rott and Sears predict separation. A substantial number of analytical investigations on the topic have already appeared as reviewed recently by Sears and Telionis [15] and Williams [16]. However the available experimental data up to now is inadequate to validate the models of unsteady separation.

The work of Vidal and Ludwig pertains only to steady flow, and the work of Despard and Miller is confined to oscillatory flows with high frequencies and Reynolds numbers. Our knowledge, therefore, about this complex phenomenon is remarkably narrow and seriously in need of more intensive investigation. This can be accomplished both by methods of flow visualization, and by hot wire anemometer techniques. Visualization methods were employed by Schraub et. al. [17] Werle [18], Ruiter, Nagib and Fejer [19] and McCroskey [20] to study unsteady viscous flow phenomena, but the specific cases considered and the scale of the models were designed for a study of the entire flow field. There was no emphasis on the features of the unsteady boundary-layer and in particular separation. In a most recent effort Carr, McAlister and McCroskey [21] employ a variety of sensing devices ranging from flow visualization methods (tufts, smoke) to pressure or velocity measuring methods (pressure transducers, hot wire anemometers etc.) to study the phenomenon of unsteady stall. In this study some basic features of unsteady separation were verified. In particular pressure and velocity signatures throughout a period of oscillation are given for different stations

on the airfoil and compared with flow visualization data.

In the present paper we report on our experimental investigations of unsteady boundary layer separation. In an effort to receive an overall picture of the phenomenon it was decided to magnify and visualize the immediate neighborhood of separation. To this end a lowspeed water tunnel was designed and constructed. Flow visualization was accomplished by dispersion of solid particles with density very close to the density of water. The method developed and described in this paper can capture approximately the instantaneous velocity field. Boundary layer velocity profiles were generated in this manner for transient and oscillatory velocity fields. Glycerin-water mixtures were used to achieve low Reynolds number flows with measureable magnitudes of velocity.

In earlier studies of visualization it was attempted to generate information about the whole flow field. As a result, the details and the mechanism of unsteady separation were not adequately revealed. In the present study, special effort is directed towards the amplification of the neighborhood of separation. In most of the flows visualized the frame of visualization is of the same order of magnitude with the boundary layer thickness. Except of the work of Despard and Miller [10], quantitative boundary layer data in the neighborhood of laminar separation are presented here for the first time. Despard and Miller concentrate in oscillatory flows. In the present paper we compare our data with those of Despard and Miller and reconfirm the validity of their definition for separation in oscillatory unsteady laminar boundary layers. The present study proceeds further in the area of transient and impulsive flows to provide data that may appear useful to numerical analysts.

2. THE VPI WATER TUNNEL

The basic specifications that the VPI water tunnel was expected to meet were: a. Test sections appropriate for studying laminar or turbulent boundary layers as well as the potential flow about simple models. Reynolds numbers based on the length of the test section should therefore range from 10^4 to 10^6 or more; b. Lowest possible volume so that expensive fluids like glycerin-water mixtures, Dow-Corning Fluid etc. could be used to fill the facility; c. Materials that would sustain corrosive fluids as for example NaCl solutions, necessary for hydrogen-bubble visualization, potassium permanganate and dilute acidic solutions for dye visualization etc. It should be noted that no permanent dyes can be used, since the working medium is usually expensive and cannot be disposed after a set of dye visualization experiments; d. Operation free of vibrations. It is imperative that vibrations from the pump and the driving motor or any device used to generate unsteady hydrodynamic effects should not be transferred to the test section; e. Total cost within the order of $15,000. This task appeared difficult to meet due to unexpected rises of material costs.

To meet these specifications the tunnel shown in Fig. 1 was designed. Long and carefully calculated diffusers were avoided in order to meet the requirements of low cost and small total volume of working medium. Synthetic materials resisting the corrosive chemicals were chosen, namely plexiglass for the test sections and the settling chamber and PVC pipes for the remaining sections of the tunnel.

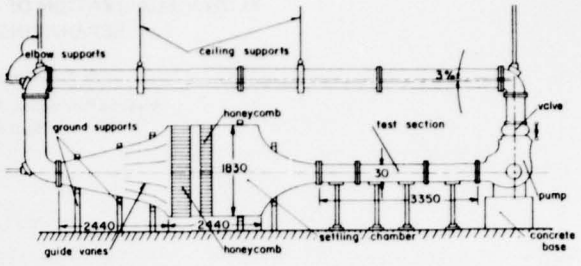

Figure 1

The VPI low speed water tunnel. All the dimensions in all figures are in mm.

A circular to rectangular converging section leads to the short diffuser and the settling chamber. (see Fig. 1) Guide vanes situated in the diffuser cut the size of large eddies and suppress separation on the walls of the diffuser. At the upstream end of the settling chamber two aluminum honeycombs are situated as shown in Fig. 1. These honeycombs are made by Hexcel-Bel Air and have hexagonal openings of approximately 3 cm^2 cross-sectional area and a diameter to length ratio equal to 12. The diffuser, the settling chamber, the converging section and the test sections are all constructed out of plexi-glass pieces of dimensions (3/4 in x 4 ft x 8 ft). A great effort was made to avoid large deflections of the side walls. This was accomplished by prestressed external steel reinforcements and transverse aluminum bolts.

The converging section leads into a 25 cm x 30 cm (10 in x 12 in) rectangular test section. The test section is made up of interchangable units of 2.7 m (9 ft) total length. In this way large Reynolds numbers with not so large velocities can be achieved. A flexible shoot leads the flow into a low-head pump. The pump is made by Bell and Gossett (model: VSCS-PF, S&D 12 x 14 x 12 1/2) and has the following basic characteristics: 12 in discharge diameter, 8 ft head, and 2000 gpm flowrate. Chrome coating of the pump housing and the impeller appeared very expensive and time consuming. Instead it was decided to have these components cold-galvanized by Livingstone Coating Co. of North Carolina. Two motors are available to drive the pump. The first is a "Marathon Electric" 1170 RPM, 230V, 15 H.P. motor which can drive the system at full speed (3m/sec). To control the speed of the tunnel a DURCO BL-311 cast iron valve with a teflon lining and a stainless steel butterfly is connected to the discharge of the pump. For the low range of velocities a 2 H.P., 220 V variable speed motor (U.S. Electrical Motors with a U.S. varidrive) is also available. This motor can drive the pump with a range of 292-1170 RPM.

Elbows, transitions from rectangular to circular sections and piping that connects the pump to the settling chamber were manufactured out of PVC (Poly-Vinyl-Chloride).

A smaller facility was also constructed as shown in Fig. 2. This is a closed circuit tunnel with a free surface above the test section. The test section is totally submerged but the driving of the flow can be accomplished through a low speed impeller at the free

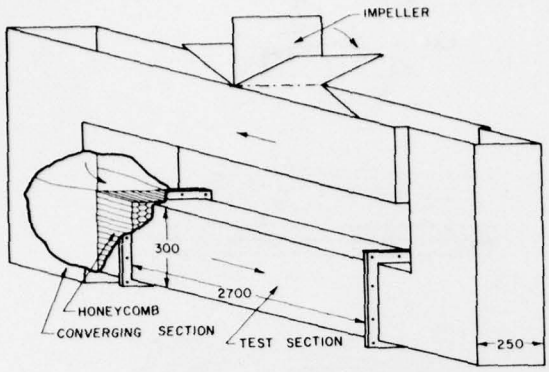

Figure 2

The free-surface water tunnel. All dimensions in mm.

surface of the facility. This tunnel offers the advantages of very small volume of contained fluid, convenient exchange of the working mediums and as a result, access to the model and the sensing devices. The same test sections from our larger facility are received and therefore, preliminary tests can be performed with the small tunnel. Both facilities were calibrated with the flow visualization methods described in the sections that follow as well as by laser anemometry.

3. THE EXPERIMENTAL LAY-OUT

To visualize the flow we use pliolite and amberlite particles* that are dispersed in the fluid. The density of these substances is respectively ρ = 1.02 and 1.05 g/cm^3. These particles are separated by sieve-screening, according to their sizes, into particles of the order of 0.1 to 0.2 mm. Pliolite particles are bright white and should be preferred because of their higher reflectivity. However, mixtures of glycerin and water are more dense than pure water and pliolite particles dispersed in such mixtures experience buoyancy forces that push them toward the top of the facility. Amberlite particles were proved more useful for experiments with glycerin-water mixtures. The particles to be used in a certain experiment are mixed in vertical columns and allowed to settle. The neutrally buoyant particles are withdrawn from the mixture, leaving behind the ones that either float to the top or sink to the bottom of the column.

The flow is visualized in planes parallel to the axis of the test section. All of the models tested are two-dimensional and the test section was scanned to check the two-dimensionality of the flow. A thin sheet of light is generated by a system of lenses as shown in Fig. 3, or by a parabolic reflector. The nearly parallel light so generated is passed through two successive slots of 5 mm width and then it is led into the test section. In front of the reflecting mirror and along the light path, a flash bulb is also situated, which may flash through the same slots into the test section.

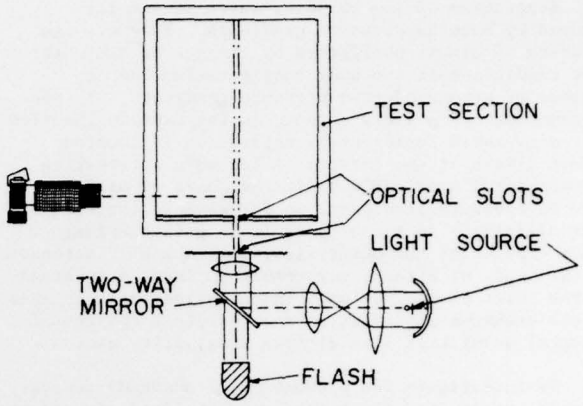

Figure 3

The optical arrangement for flow visualization.

Still pictures are taken with a 35 mm Olympus Camera and a 90 mm, f 2.8 Vivitar Macro Lens. Time exposures of 1/2 up to 1/120 sec are used. The images of particles expose the film over the time exposure interval by segments proportional to the average local velocity. This method of course has some limitations. The larger the speed of a particle, the shorter time its image exposes the film at a certain point and therefore the contrast is reduced. This drawback could be compensated only if a very powerful source of light is used. It was also discovered that the method is not appropriate for recording flow fields with both large and small velocities. The proper camera speed is determined by the order of magnitude of the velocities that are expected in the region of interest. If a camera speed is chosen to reveal a small-velocity field then the faster moving particles expose almost the entire width of the film and it is impossible to measure the lengths of individual path segments. Moreover the direction of the instantaneous velocity cannot be calculated with accuracy, since for unsteady flows the particle paths do not coincide with the instantaneous streamlines of the flow. Finally, the most important criticism may arise from the fact, that for large accelerations of the flow and for long time exposures (1/2, 1/4 sec.), the average velocity may be very far from the instantaneous velocity. For all the experiments performed, this effect was carefully considered and the error involved was estimated. A typical length for changes due to unsteady diffusion is the quantity $L_d = \nu t$ whereas the path traveled by a particle in the same period of time is $L_p = Ut$. The ratio of the two lengths $L_d/L_p = (\nu/U^2 t)^{1/2}$ is a dimensionless number indicative of the relative order of changes due to unsteady diffusion and convection. The smaller this number, the more accurate the representation of the unsteady flow by the present method. In our experiments this number was kept below the value of 0.05.

*Pliolite is the commercial name of polyvinyltoluene butadiene, made by Goodyear Chemicals.

Amberlite is the commercial name of a white ion exchange resin, IRA-93 made by the Rohm and Haas Company.

With the opening of the camera shutter, a flash may be triggered to direct an intense beam of light through the same optical path. (see Fig. 3) In this way the beginnings of particle path segments are marked on the film with brighter spots. This technique is particularly helpful if reversing flows are to be examined.

Separation of the boundary layer is usually induced by adverse pressure gradients. However, its location is almost unaffected by changes of the outer flow conditions if the body configuration induces regions of strong adverse pressure gradients. In the extreme case of a sharp corner, as for example the flow over a backward facing step, separation is located almost always at the corner. A lot more interesting for practical applications are the cases of mild adverse pressure gradients, as for example the flow over airfoils. In these cases it is possible that minor changes of the outer flow, like a small increase of the angle of attack, may result in large excursions of the point of separation. This implies large changes of the pressure distribution and therefore changes of integral quantities like airfoil drag, lift, etc.

To investigate the phenomenon of unsteady separation it was decided first to design an ideal situation, where for steady flows, two distinct locations of separation at points say I and II could be achieved. The flow would then be forced to readjust from conditions I to conditions II impulsively, or in a transient manner or continuously, back and forth between I and II, in an oscillatory fashion. To this end a circular section with dimensions given in Fig. 4 is attached at the bottom of the test section. This model is made out of plexiglass, to permit lighting of the flow on its surface. It will be referred to in the sequel as model A. A 7 mm deep hole was drilled and later filled with epoxy, to provide a length scale. This is shown in almost all of the flow visualization pictures that follow. It was later used to calculate the lengths of particle path segments as well as to define the axial coordinates on the skin of the body. The boundary layer is allowed to grow on the bottom wall of the test section. It is then led over a small accelerating region, at the forward portion and towards separation at the lee side of our model. Separation is controlled by a flap as shown in Fig. 4. Two positions of the flap are found that, for steady flow, correspond to two distinct locations of separation, positions I and II shown schematically in Fig. 4.

Experiments were also performed with a second model which essentially represents smoothing of the contours and hence pressure gradients of the circular arc just described. The dimensions of this model, referred to in the sequel as model B, are given in Fig. 5. The afterbody of this model is adjustable, thus permitting minor changes in the values of the adverse pressure gradient.

The experiments described in this paper correspond to flows over fixed surfaces, while unsteadiness is introduced via outer flow pressure distributions. The continuation of this effort, to be reported later, involves experiments with moving surfaces. In the first category we simulate changes of the airfoil environment due to gusts or outer flow disturbances. The second category corresponds to changes of the angle of attack of an oscillating blade.

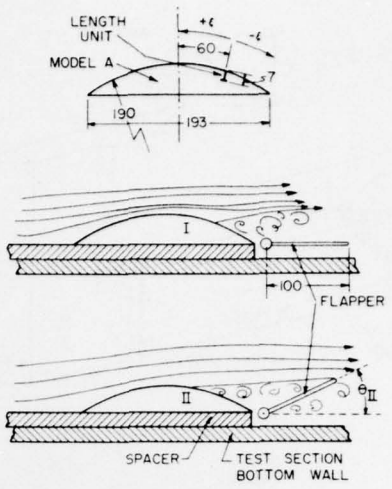

Figure 4

Circular arc model (model A) and schematic of the flap positions and streamline configurations for conditions I and II. All dimensions in mm.

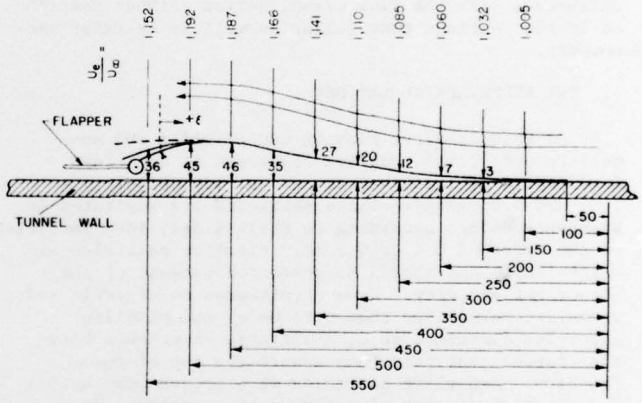

Figure 5

Smooth-pressure-gradient model (model B). All dimensions in mm.

4. TRANSIENT AND IMPULSIVE CHANGES OF THE PRESSURE DISTRIBUTION

In the first phase of our experiments, using model A and water as a medium, we examine the case of impulsive changes of the flow. To this end,the flap is connected to a lever and a strong spring. With the release of the lever a microswitch is activated and a flap quickly moves from position I to position II. A simple system of electronics is used to activate the camera and the flash. This was first accomplished using the delay-circuit as shown in Fig. 6 to control the opening and the closing of the camera's shutter. The time delay, Δt, between the initiation of the phenomenon and the opening of the shutter is controlled and the experiment is repeated with different Δt in order to receive the sequence of unsteady velocity

fields. This system has a clear disadvantage. A sequence of photographs thus generated does not correspond to different instances of the same transient phenomenon, spaced apart by equal time intervals. It represents, instead, the flow field of repetitions of the same transient phenomenon, viewed at different instances after its initiation. The repeatability of the flow is therefore an important factor and in fact some of the sequences of photographs thus received indicate discontinuities.

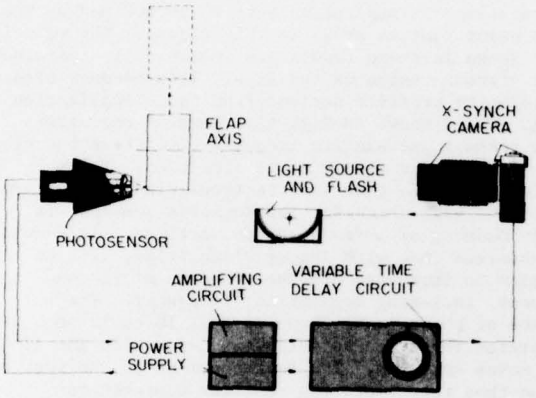

Figure 6

Electronic circuit for triggering the disturbance generator and the camera.

One set of experiments was performed with model A, $R_e \simeq 10^4$ and a sharp change of the flap inclination from $\theta_I = 0$ to $\theta_{II} = 40°$. In Fig. 7 we show four visualizations of the flow at times t = 0.2, 0.4, 0.6, and 0.8 sec. after the initiation of the impulsive change, taken with a camera speed of 1/8 sec. The sequence in Fig. 7 indicates that the location of separation, moves slowly upstream. The initial station of separation is marked in these plates by the Symbol S_1 and the instantaneous station of separation defined by the wake formation, is marked by an arrow. However, upstream of the point of separation, there exists a relatively thin region of reversed flow, in qualitative agreement with the descriptions of Sears and Telionis [15], Carr, McAlister and McCroskey [21] et. al. (see review article of Telionis, [22]). The reversed direction of the flow is apparent from the bright dots that mark the particle location at the beginning of the film exposure.

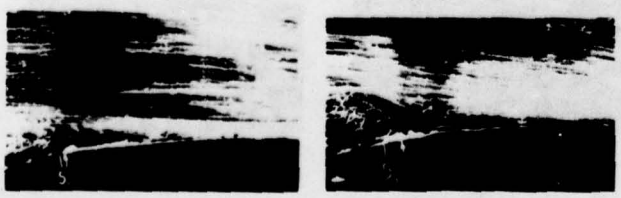

t = 0.2 sec. t = 0.4 sec.

t = 0.6 sec. t = 0.8 sec.

Figure 7

Flow visualization of upstream moving separation over model A, for impulsive change $\theta_I = 0$ to $\theta_{II} = 40°$ and $R_e = 10^4$.

In Fig. 8 we show dye visualization of the same phenomenon. Dye is emmitted here approximately 10 mm downstream of the location of steady separation and it is seen to creep upstream, underneath the laminar boundary layer.

t = 0.2 sec. t = 0.5 sec.

Figure 8

Dye visualization for the flow of Fig. 7.

A very interesting feature of the flow is apparent from both particle and dye visualization. The separated region grows at the beginning in a controlled fashion but after a certain time it appears as if it attains momentum and its thickness increases abruptly. The phenomenon is reminiscent of the bursting of the leading edge separation bubble. This is clearly shown in the last frame of Fig. 7. The momentum thus generated takes quickly the form of a well organized vortex. The weak turbulent field of the wake is probably still present but the dominant motion appears clearly to be the vortical motion and the exchange of mass with the outer stream which is accomplished further downstream. This trend appears to persist in all the experiments performed and it is documented in many sequences of still frames some of which are contained in Ref. 23.

Experiments performed with smaller Reynolds numbers indicate a characteristically different behavior. Such experiments were performed in the smaller facility, (Fig. 2) with a mixture of glycerin and water in a ratio 60% by volume. The use of glycerin mixtures permits one to reduce the Reynolds numbers without simultaneous reduction of the velocities. It is therefore easier to observe the flow and capture a velocity field with a reasonable film exposure time. Examination of low Reynolds number flows using water as a testing medium would require very small velocities and unrealistically small Δt's. However, the use of

glycerin has some distadvantages as well. The dimensionless number $L_d/L_p = (\nu/U^2t)^{1/2}$ which describes the ratio of distances of diffusion propagation to particle displacement, grows. As a result, the error involved when using the present method becomes larger. In the experiments performed with glycerin-water mixtures, L_d/L_p ranged between 0.05 and 0.12.

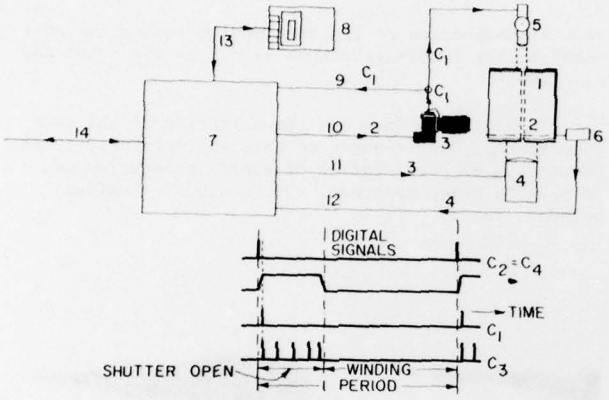

Figure 9

The triggering system interfaced with a microprocessor: 1) test section with transparent walls (cross section); 2) plane of light (observation plane); 3) OLYMPUS OM-1 motor drive camera (3 frames per second) with VIVITAR 90mm f2.8 MACRO LENS (1:1 magnification ratio); 4) fast recycling XENON strobe (up to 20 flashes per second) combined with continuous output 1000W Quartz lamp in the same housing and focused at infinity by a lens; 5) VIVITAR 283 STROBE (up to 3 flashes per second) focused at infinity by a lens; 6) oscillator (variable speed motor, oscillating shaft); 7) KIM-1 (MOS) microprocessor (6502 ARRAY) with two 6530 arrays (ROMS), 1152 bytes of "read" "write" memory, two programmable interval timers, six LED display, keyboard, audio cassette interface, TTY interface; 8) audio cassette recorder interfaced with the microprocessor; 9) camera's shutter open feedback through cameras X SYNCH and slow strobe's (5) control line; 10) motor drive control line; 11) fast strobe's (4) control line; 12) R.P.M. 2 phase feedback through a LED/photosensor; 13) audio cassette interface; 14) TTY interface with IBM computer (optional).

Transient flows are investigated again for low Reynolds numbers. A more sophisticated triggering system is now being used. It involves a KIM-1 microprocessor (see Fig. 9) which is programmed to receive the signal of the initiation of the impulse and then activate the flash and trigger the camera at specified intervals of time. In this way it is possible to receive snapshots of the same phenomenon at different times and thus capture the evolution of one single unsteady flow field. In Fig. 10 we show a sequence of velocity fields taken with a camera speed of 1/2 sec. and a Reynolds number equal to 1000. The first frame represents the steady flow for $\theta = 0$. The second frame is shot with a delay $\Delta t_o = 0.5$ sec. after an impulsive change of the flap angle from $\theta = 0$ to $\theta = 40°$. The following frames were received at intervals of $\Delta t = 1$ sec. The speed of exposure was kept rather low in order to reveal the properties of slow moving flow at the bottom of laminar boundary layer and in the separated region. Immediately after the initiation of the impulsive change, the flow indicates a violent departure from the steady state configuration. Very soon, two distinct recirculating regions appear and a saddle point configuration is formed at approximately the station where steady separation occured. These flow patterns could be interpreted as reversed flow upstream of separation, if separation were to be defined as the saddle point that is shown in this figure. The velocity fields shown in these frames are indeed fully contained in the viscous region of the flow. This becomes clear from velocity profiles derived from the visualization of Fig. 10 and shown in Fig. 11. However the first bubble seems to retain its identity even after the flow has arrived at its steady state condition. It is therefore possible that such recirculating bubbles are part of the wake which for low Reynolds numbers, is usually made up of a few discrete vortices. It should be emphasized that with larger viscosities, viscous diffusion is increased and the response of viscous phenomena, including separation, is faster. The sequence of photographs shown in Fig. 10 could be interpreted therefore as follows. Separation immediately moves upstream. The rearrangement of the vortices in time then represents the familiar unsteadiness contained in the wake. This would be the interpretation that the numerical analyst would probably offer (Mehta and Lavan, [24] Mehta, [25]). Indeed, for low Reynolds numbers reversing of the flow direction could be defined as separation.

In Fig. 12 we show a sequence of velocity fields again for $R_e \tilde{=} 1000$ but with a final flap inclination $\theta_{II} = 30°$. The general characteristics of the flow are similar. In fact it is now easier to accept that the leading recirculating bubble is part of the attached

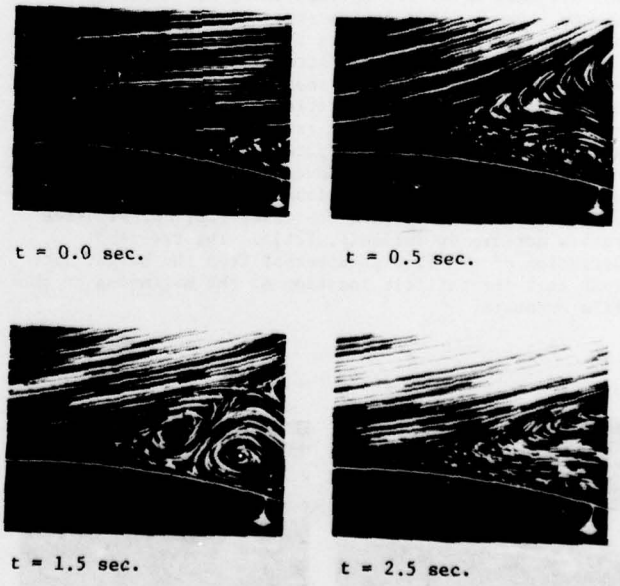

t = 0.0 sec. t = 0.5 sec.

t = 1.5 sec. t = 2.5 sec.

Figure 10 continued on the next page

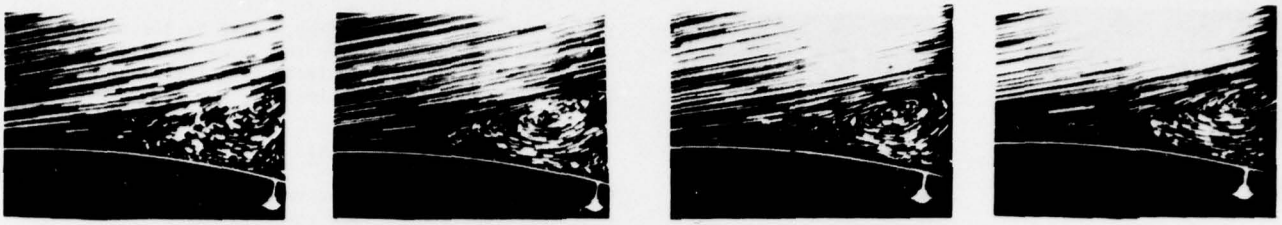

t = 3.5 sec. t = 4.5 sec t = 1.5 sec. t = 2.5 sec.

Figure 10

Flow visualization of instantaneous velocity fields over model A for an impulsive change $\theta_I = 0$ to $\theta_{II} = 40°$ and $R_e = 10^3$.

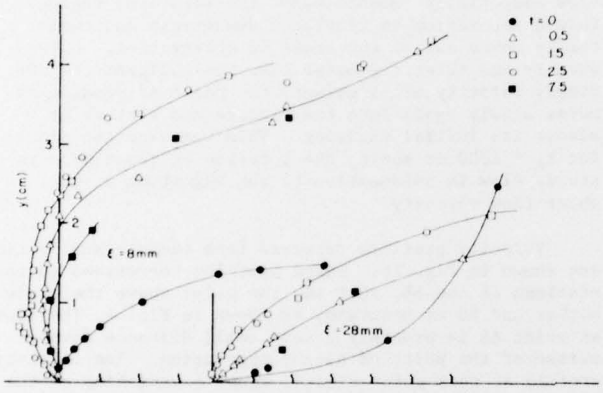

Figure 11

Velocity profiles at stations $\xi = 8$ and $\xi = 28$ (see Fig. 4), derived from the flow visualization of Fig. 10.

boundary layer. It appears quite possible and in fact our experimental data seem to support this idea, that with growing Reynolds numbers, the flow patterns shown in Figs. 10 and 12 are conserved but their dimension perpendicular to the wall shrinks together with the laminar boundary layer. If this is true it would imply that the patterns of Fig. 11 and 12 represent the recirculating flows in front of an upstream moving separation as described by Sears and Telionis [15] and Despard and Miller [10].

t = 3.5 sec.

Figure 12

Flow visualization of instantaneous velocity fields over model A for an impulsive change $\theta_I = 0$ to $\theta_{II} = 30°$ and $R_e = 10^3$.

Experiments with water ($R_e \simeq 10^5$) were repeated for transient flows using the triggering system shown in Fig. 7 and model B which provides milder pressure gradients. The sequence of frames shown in Fig. 13 was received with an initial delay $\Delta t_o = 1$ sec. and subsequent time intervals $\Delta t = 1$ sec. These plates represent average flow fields of the same phenomenon which is developing in time. In the blow up of one of these frames the very thin layer of reversed flow predicted theoretically in Ref. 26, is clearly shown. Fig. 14 shows a sequence of velocity profiles at $\xi = 0$. These profiles correspond to the initial steps of the motion during which the flow is well ordered and the wake appears in the form of a recirculating bubble. The sequence of plates of Fig. 13 indicates that at t = 4 sec. a spectacular explosion occurs in the wake and the particles of the wake, including the ones that reside next to the wall are jettisoned into the flow. Subsequently this erratic motion subsides and the configuration approaches the steady flow that corresponds to the final flap angle.

t = 0.0 sec. t = 0.5 sec. t = 0 sec. t = 1 sec.

Figure 13 continued on next page

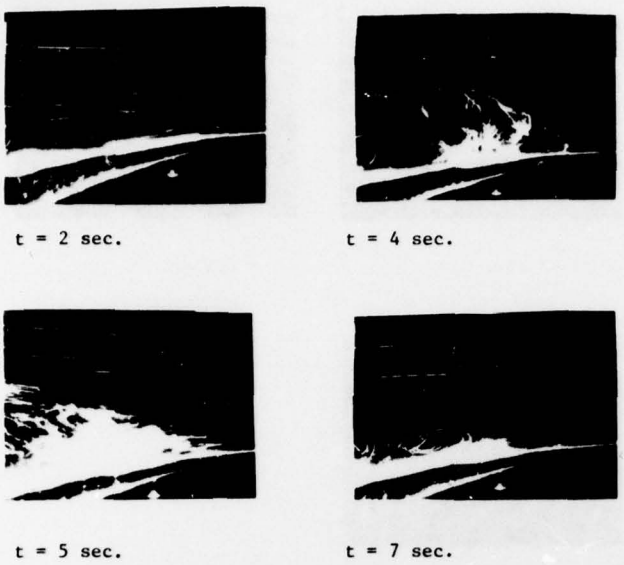

t = 2 sec. t = 4 sec.

t = 5 sec. t = 7 sec.

Figure 13

Flow visualization of instantaneous velocity fields over model B for an impulsive change $\theta_I = 0$ to $\theta_{II} = 30°$ and $R_e = 10^5$.

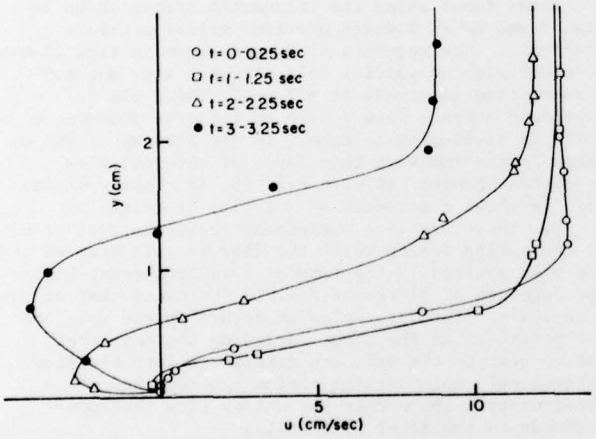

Figure 14

Velocity profiles at station $\xi = 15$ derived from the flow visualization of Fig. 13.

5. SEPARATION OVER A FIXED SURFACE WITH OUTER FLOW ACCELERATIONS

In another set of experiments we studied the response of laminar separation to accelerating and decelerating outer flows, for $R_e \simeq 1000$ In these experiments the disturbing flap was completely removed and unsteadiness was introduced only via the change of the magnitude of the outer flow. It should be noted here that potential flow is unaffected by such changes and the streamline configuration of inviscid flow should remain undisturbed. The flow is governed by Laplace's equation

$$\nabla^2\phi = 0$$

with ϕ the potential function. Time is introduced via the boundary conditions, in this case the free stream velocity. However, in inviscid flow the pressure is given by Bernoulli's equation

$$\frac{\partial\phi}{\partial t} + \frac{V^2}{2} + \frac{dp}{\rho} = f(t)$$

where V, p and f(t) are the velocity, pressure and an arbitrary function of time respectively. Clearly time variations of ϕ generate pressure disturbances which in turn influence to location of separation.

In Fig. 15 we show a sequence of velocity fields for a flow accelerating from $U_\infty = 12$ cm/sec. to $U_\infty = 25$ cm/sec. The visualization at t = 0 corresponds to the undisturbed flow. The flow at an initial interval $\Delta t_o \simeq 0.5$ and subsequent intervals $\Delta t = 1$ sec. after the initiation of the acceleration is shown until $\Delta t = 3.5$ sec. An inspection of the outer flow is enough to convince that during the acceleration process the outer flow essentially "washes away" the separated region. Indeed separation is displaced downstream and eventually moves out of the frame of observation. Subsequently and after the outer flow has achieved the new steady velocity of 25 cm/sec, the point of separation moves slowly again into the picture and arrives at almost its initial position. This was expected since for $R_e \simeq 1000$ or above, the location of separation in steady flow is insensitive to the magnitude of the outer flow velocity.

Velocity profiles received from these visualizations are shown in Fig. 16. These profiles correspond to the stations AA and BB, that is, the point above the scale marker and 60 mm upstream, as shown in Fig. 4. The flow at point AA is probably a very small distance downstream of the point of steady separation. The velocity profile at this point clearly shows a vanishing of the skin friction, or perhaps a small region of slow reversed flow. After the acceleration of the outer flow begins, the wall shear becomes positive and

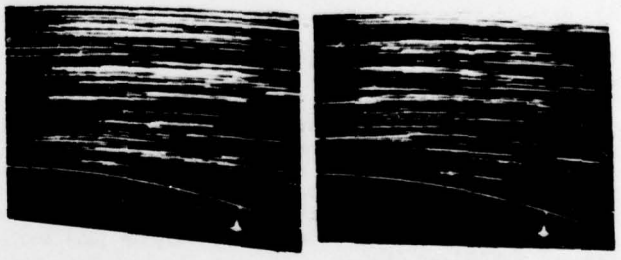

t = 0 sec. t = 0.5 sec.

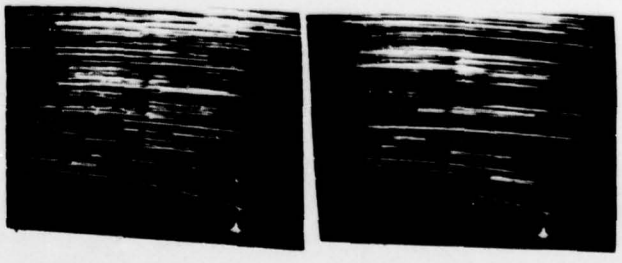

t = 1.5 sec. t = 2.5 sec.

Figure 15 continued on next page

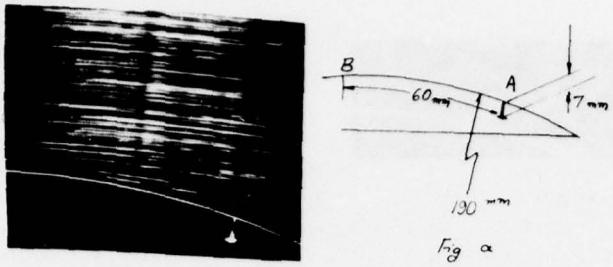

t = 3.5 sec.

Figure 15

Flor visualization for flow over model A accelerating in magnitude from U_∞ = 12 cm/sec to U_∞ = 25 cm/sec.

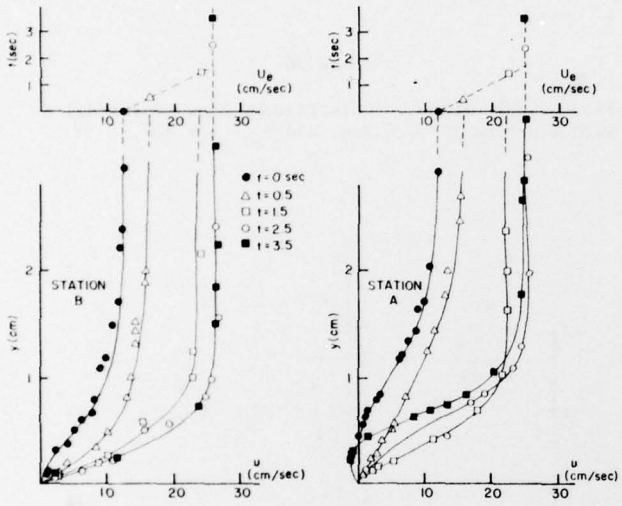

Figure 16

Velocity profiles at stations ξ = 0 (station AA) and ξ = 60 (station BB) (see Fig. 4) derived from the flow visualization of Fig. 15.

increases sharply. The inflection point of the profile disappears and only after the outer flow achieves its final value, we observe a sharp decrease of the velocity, the appearance of a point of inflection and a vanishing value of the velocity at the same distance from the wall as for t < 0. Normalized velocity profiles are shown in Fig. 17.

A sequence of instantaneous velocity fields for decelerating flows is shown in Fig. 18. In this case the point of separation is displaced sharply upstream, while the separated region thickens abruptly. As time grows the flow pattern returns again to its original configuration.

A plot of the excursions of separation for accelerating and decelerating flows is shown in Fig. 19. In the same figure we show the variations of the outer flow for comparison. It appears that the time scale of the response of separation is of the same order of magnitude with the scale of changes of the outer flow. Experiments repeated with much smaller accelerations resulted in weaker displacements of the point of separation, until no effect at all could be observed.

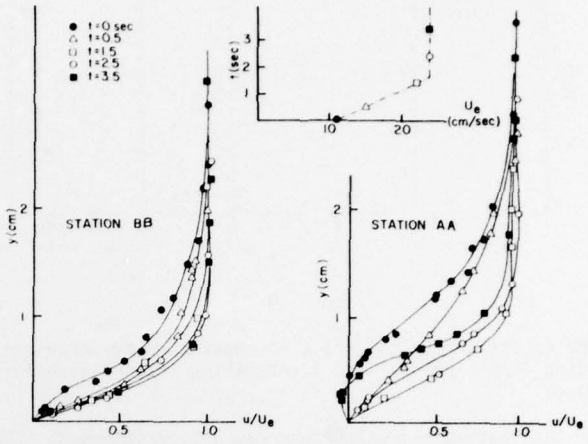

Figure 17

Dimensionless velocity profiles for stations AA and BB derived from the data of Fig. 16.

t = 0.5 t = 1.5 sec.

t = 2.5 sec. t = 3.5 sec.

Figure 18

Flow visualization for flow over model B decelerating in magnitude from U_∞ = 20 cm/sec. to U_∞ = 12 cm/sec.

6. PERIODIC DISTURBANCES OF THE OUTER FLOW

In the present paper we report only on some preliminary findings in the area of oscillatory flows. Disturbances are again generated via flaps of different sizes in the downstream end of the models as shown in Fig. 4. The flap is driven by a variable speed motor via pushing rods in the shape of a parallelogram. In this way, no external unbalanced forces are transmitted and the test section is free of vibrations. The mechanism that drives the parallelogram is a classical crank-connecting rod system with a relatively long rod,

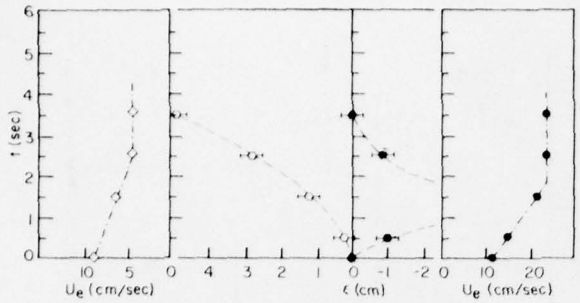

Figure 19

The excursions of the point of separation for accelerating (open symbols) and decelerating (closed symbols) flows.

so that harmonic oscillations can be approximated. The range of frequencies thus accomplished is 0.5 - 30 Herz. Experience derived from the present experiments and earlier analytical and experimental investigations indicates that separation responds to unsteady disturbances with a characteristic inertia-like behavior. It was thus expected that the domain of interest would rather be in the lower part of the range of frequencies.

The triggering device of Fig. 9 is used to signal all the events. A photosensor receives a signal at a specified phase of the rotating disk which drives the flap (see point 6 in Fig. 9). This message is fed into the microprocessor, which in turn sends a signal to the camera (line 10) after a delay time Δt, after one cycle is completed. Thus, during this nth cycle, the signal arrives at the camera delayed by $n\Delta t$. If the quantity $n\Delta t$ exceeds the period of oscillation, then the process is repeated starting from zero delay. In this way measurements are taken at different phases of the periodic motion.

Figure 20 shows a sequence of averaged velocity fields of a flow oscillating with a period T = 0.6 sec. and an average Reynolds number $R_e = 5 \times 10^5$. Measurements were received for $\Delta T = 0.1$ sec. The film exposure time was 1/15 sec. At t = 0 the flap angle was $\theta = 0$. A phase delay of approximately 60° is apparent. The separated region appears to gain momentum and its thickness increases sharply. A relatively violent vortex is in fact propagating from downstream until it engulfs the whole wake. However the location of separation is barely affected by the oscillatory motion and remains approximately at the position $\xi = 15$ mm, that is two unit lengths upstream of $\xi = 0$.

t = T/6 t = 2T/6

t = 3T/6 t = 4T/6

t = 5T/6

Figure 20

Flow visualization for oscillatory flow over model A with a period T = 0.6 sec. and $R_e = 5 \times 10^5$.

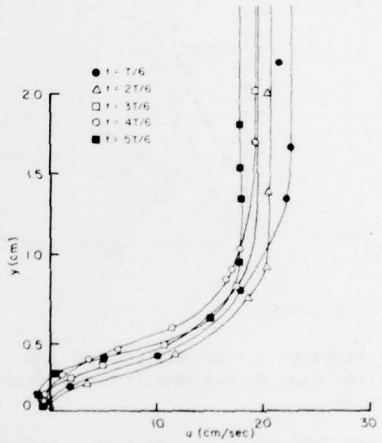

Figure 21

Velocity profiles of the flow of Fig. 20 at $\xi = 15$ mm.

Velocity profiles received at the point of separation as detected from the flow visualizations are shown in Fig. 21. In this figure it is clear that the wall shear fluctuates between the zero and a negative value. It is therefore concluded that for the case considered, the criterion proposed by Despard and Miller [10] is met.

The displacement of separation from its steady state position that corresponds to the $(\theta_{II} - \theta_I)/2$, is shown in Fig. 22. This figure indicates that in all cases examined the point of separation is displaced further downstream as the frequency increases. In fact for frequencies of the order of $\omega = 10$ Herz, separation disappears completely from the models examined in this study. Comparison with the experimental data of

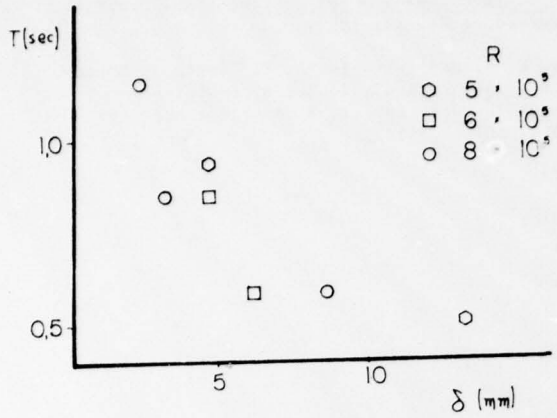

Figure 22

The downstream displacement of the point of separation.

Despard and Miller was not possible because of the differences in the range of frequencies examined.

7. CONCLUSIONS

The present paper is the first formal report on an experimental investigation undertaken three years ago. It describes very briefly the facilities we designed and constructed and the experimental methods we developed. The main thrust of our effort was directed towards the development of effective and accurate methods of flow visualization, capable of supplying qualitative as well as quantitative information. Our target is unsteady viscous flows and both these characteristics pose particularly irksome difficulties.

The flow visualization method developed, unlike the method of smoke visualization or the hydrogen bubble technique, is nonintrusive. It provides the capability to visualize without special provision, any part of the flow and permits the detection of forward or reversed flow. Moreover, the method is applicable to viscous or inviscid as well as to laminar or turbulent flows.

The ultimate goal of this effort is the investigation of unsteady laminar separation. All experiments were performed with rigid and fixed solid surfaces. Various models were tested that correspond to varying values of adverse pressure gradients. Time dependent disturbances of the outer flow pressure distributions were accomplished using downstream flaps or accelerations and decelerations of the mean flow.

A characteristic inertia in the response of separation was observed in the experiments performed. For impulsive changes of the outer flow the order of magnitude of the time required for the flow to arrive at its new flow pattern is L/U_∞. Separation is usually detected by an abrupt thickening of the wake. An upstream moving separation is preceded by a thin layer of reversed flow. On occasions this layer was found to be as thin as 1% of the thickness of the boundary layer. However, even then, methods that detect separation by measuring the wall shear directly would fail to predict the phenomenon in unsteady flow.

The present investigation of actual streamline patterns and wake shapes indicates that the problem is more complex than was originally conceived. For mild adverse pressure gradients which should be the case in flows over thin airfoils, the separated region is so thin that the point of flow reversal can be easily confused with the point of separation. Pressure variations would not be greatly affected by separation and perhaps the argument and the controversy over the proper definition of separation in this case looses its meaning.

One of the most interesting findings of the present study is that a considerable time after an impulsive change has been imposed the separated region appears somehow to gather momentum and eventually erupts into a violent motion which may later develop in a strong and well ordered vortex. Subsequently this activity subsides and the flow returns to its steady state pattern.

The study of accelerating or decelerating outer flows indicates a strong influence on separation. A uniform acceleration essentially "washes away" separation altogether, whereas deceleration pushes separation upstream. After a small interval of time, separation slowly returns to its original position.

Preliminary work with oscillatory flows resulted in conclusions similar to those of Despard and Miller. Separation is not affected by the amplitude of oscillation but responds quickly to changes of the frequency of oscillation. The criterion proposed by Despard and Miller is met with reasonable accuracy. However for the low range of frequencies and the configuration of the models examined, the point of separation is shifted downstream of its quasi-steady location. Perhaps this is due to the fact that our outer flow velocity spatial distribution varies with time, a situation that corresponds to a pitching airfoil, whereas Despard and Miller generated disturbances only in the magnitude of the outer flow.

ACKNOWLEDGEMENTS

Research sponsored by the U.S. Army Research Office under Grant No. DAHC04-75-G-0067

REFERENCES

1. Prandtl, L., "Uber Flussigkeitsbewegung bei sehr kleiner Reibung", Proc. Intern. Math. Congr. Heidelberg, 484-91, 1904.

2. Sears, W. R., "Some Recent Developments in Airfoil Theory", J. Aero. Sciences, 23, 490-499, 1956.

3. Moore, F. K., "On the separation of the Unsteady Boundary Layer", Boundary Layer Research, H. Görtler, ed. Springer, Berlin, 296, 1958.

4. Rott, N., Unsteady Viscous Flow in the Vicinity of a Stagnation Point, Quart. Appl. Math. 13, p. 444, 1956.

5. Rott, N., Theory of Time Dependent Laminar Flows, in Theory of Laminar Flows, F. K. Moore (ed.), Princeton University Press, Princeton, N.J., 1964.

6. Vidal, J. R., "Research on Rotating Stall in Axial-Flow Compressors, Part III", WADC TR-59-75, 1959.

7. Ludwig, G. R., "An Experimental Investigation of Laminar Separation From a Moving Wall", AIAA Paper 64-6, 1964.

8. J. S. Tennant, "A Subsonic Diffuser with Moving Walls for Boundary- Layer Control", AIAA J. 11, 240-242, 1973.

9. Tennant, J. S. and Yang, T., "Turbulent Boundary-Layer Flow from Stationary to Moving Surfaces" AIAA J., 11, 1156-1160, 1973.

10. Despard R. A. and Miller, J. A., "Separation in Oscillating Laminar Boundary-Layer Flows", J. Fluid Mech., 47, 21-31, 1971.

11. Sandborn, V. A., "Characteristics of Boundary Layers at Separation and Reattachment", Res. Memo. No. 14, College of Engineering, Colorado State University, 1969.

12. Simpson, R. L. "Features of Unsteady Turbulent Boundary Layers as Revealed from Experiments", in Unsteady Aerodynamics, AGARD PREPRINT No. 227, paper No. 19, 1977.

13. Kenison, R. C., "An Experimental Study of the Effect of Oscillatory Flow on the Separation Region in a Turbulent Boundary Layer", in Unsteady Aerodynamics AGARD PREPRINT No. 227, paper No. 20, 1977.

14. Telionis, D. P., and Werle, M. J., "Boundary-Layer Separation from Downstream Moving Boundaries", Journal of Applied Mechanics, 95, 389-374, 1973.

15. Sears, W. R. and Telionis, D. P., "Boundary-Layer Separation in Unsteady Flow", S.I.A.M. J. of Appl. Math. 28, 215-235, 1975.

16. Williams, III, J. C., Incompressible Boundary-Layer Separation, in Annual Review of Fluid Mechanics, Annual Reviews Inc., 9, 113-144, 1977.

17. Schraub, F. A., Kline, S. J., Henry, J., Rumstadler, P. W., and Littel, A., "Use of Hydrogen Bubbles for Quantitative Determination of Time Dependent Velocity Fields in Low-Speed Water Flows", J. of Basic Eng., 87, 429-444, 1965.

18. Wérlé, H. "Hydrodynamic Flow Visualization" in Annual Review of Fluid Mechanics, 5, 1973.

19. Ruiter, G. H., Nagib, H. M., and Fejer, A. A., "Unsteady Boundary-Layer Separation over Oscillating Airfoils", Proceedings of SQUID Workshop, Atlanta, ed., Marshall, F. J., pp. 423-425, 1971.

20. McCroskey, W. J., "Dynamic Stall on a Helicopter Rotor Blade", Proceedings of SQUID Workshop, Atlanta, ed., Marshall, F. J., pp. 346-350, 1971.

21. Carr, L. W., McAlister, K. W. and McCroskey, W.J., "Analysis of the Development of Dynamic Stall Based on Oscillating Airfoil Experiments", NASA TN D8382, 1977.

22. Telionis, D. P., "Unsteady Boundary Layers-Attached and Separated", in Unsteady Aerodynamics, Proceedings of an AGARD Symposium, Paper No. 17, 1977.

23. Telionis, D. P. and Koromilas, C. A., "Experimental Investigation of Unsteady Separation", VPI & SU Engineering Report, in press.

24. Mehta, U. B. and Lavan, Z., "Starting Vortex, Separation Bubbles and Stall, a Numerical Study of Laminar Unsteady Flow aroung an Airfoil, J. Fluid Mechanics, 67, 227-256, 1975.

25. Mehta. U. B., "Dynamic Stall of an Oscillating Airfoil, in Unsteady Aerodynamics, AGARD Preprint No. 227 Paper No. 23, 1977.

26. Sears, W. R. and Telionis, D. P. "Unsteady Boundary-Layer Separation", in Recent Research of Unsteady Boundary Layers, E. A. Eichelbrenner (ed.) 1, 404-447, 1971.

reprinted from

Nonsteady Fluid Dynamics
Edited by D. E. Crow and J. A. Miller, 1978

published by

THE AMERICAN SOCIETY OF MECHANICAL ENGINEERS
345 East 47th Street, New York, N.Y. 10017
Printed in U.S.A.